

Assessment of entanglement risk to marine megafauna due to offshore renewable energy mooring systems

Violette Harnois^a, Helen CM Smith^a, Steven Benjamins^b, Lars Johanning^a

V.Harnois@exeter.ac.uk

+0044 (0)1326 259308

^a College of Engineering, Mathematics and Physical Sciences

Renewable Energy

University of Exeter, Cornwall Campus, Cottage 2

Penryn, Cornwall TR10 9FE, UK

H.C.M.Smith@exeter.ac.uk

L.Johanning@exeter.ac.uk

^b SAMS (Scottish Association for Marine Science)

Oban, Argyll, Scotland, PA37 1QA, UK

Steven.Benjamins@sams.ac.uk

Abstract: This paper defines a methodology to compare different offshore renewable energy (ORE) mooring configurations in terms of the risk of entanglement they present to marine megafauna. Currently, the entanglement of large marine animals is not explicitly considered in environmental impact studies. Recommendations need to be developed, assessing the risk of entanglement of ORE mooring configurations at the beginning of their design process.

Physical parameters of the mooring system affecting the relative risk of entanglement have been identified as tension characteristics, swept volume ratio and mooring line curvature. These have been investigated further through six different mooring configurations: catenary with chains only, catenary with chains and nylon ropes, catenary with chains and polyester ropes, taut, catenary with accessory buoys, taut with accessory buoys.

Results indicate that the taut configuration has the lowest relative risk of entanglement, while the highest relative risk occurs with catenary moorings with chains and nylon ropes or with catenary moorings with accessory buoys. However, the absolute risk of entanglement is found to be low, regardless of the mooring configuration. This methodology can also be applied to other mooring configurations, arrays or power cables.

Keywords Entanglement, Mooring system, Offshore renewable energy, Marine megafauna, Environmental impact assessment

Highlights

- Comparison of the risk of entanglement of marine megafauna for ORE mooring systems
- Parameters: tension characteristics, swept volume ratio and mooring line curvature
- Case study with 6 mooring configurations commonly used for floating ORE devices
- Catenary moorings and moorings using accessory buoys: higher risk of entanglement
- The overall risk of entanglement is low

1. Introduction

Floating offshore renewable energy (ORE) technologies, which include most wave and some tidal devices, are undergoing extensive development and testing but are yet to reach full commercialisation. The offshore wind industry is also moving towards the deployment of floating turbines to enable a move into deeper water. A number of individual full-scale devices have been successfully deployed and the number of floating offshore renewable energy projects, and the array sizes proposed, are growing. One of the many challenges facing developers wishing to test a single device or to deploy an array is the need to ensure that these devices do not adversely impact the marine environment, or, where this is unavoidable, that such impacts are minimised and mitigated against. Although requirements differ slightly between countries, most proposed deployments require environmental impact studies. Guidelines for the implementation of such environmental impact assessments for marine energy are detailed for example in the EquiMar protocols [1]. With so few devices having undergone testing at sea, it will only be possible to validate the predicted environmental effects once devices have been in place for a number of years.

This paper considers one aspect of environmental impact assessment: the potential for entanglement of marine megafauna (e.g. cetaceans, pinnipeds, sea turtles, large sharks, etc.), between mooring lines of floating offshore renewable energy devices. Entanglement can be defined as the inadvertent capture or restraint of marine animals by strong, flexible materials of anthropogenic origin. Bycatches by lost or discarded fishing gears entangled in moorings are not considered in this study.

The consequences of entanglement are loss of animal life - possibly from endangered species- and negative public opinion. Entanglement has been observed (albeit infrequently) for large whales in stationary trap fisheries [2] and in aquaculture [3-4]. It could be noted that no entanglement has been reported in oil and gas moorings (which however does not mean it did not occur). Smaller animals are more likely to become entangled in fishing gears, for example pinnipeds (seals and sea lions) [5], or large sharks and rays [6-7]. It should be noted that entanglement is difficult to detect because it occurs offshore and underwater in remote locations with few, if any, observers.

At present, entanglement is not addressed as standard in environmental impact assessment (EIA) studies, and there are currently no records of such entanglement occurring at any offshore renewables site; however the risk of entanglement of marine mammals and turtles in moorings for wave energy devices has been raised [8]. An additional consequence of entanglement in the case of an ORE device would be a possible damage to an ORE device leading to a change in the performance of the mooring or the device.

In addition to requirements for environmental impact assessments, ORE moorings have their technical requirements, which have certain commonalities with conventional mooring systems, used, for example, for oil and gas platforms [9]. The key aspect is the need to keep the floating structure in position. In some cases, the restraint of the dynamic motion of the floating structure is additionally required, for example for floating wind or overtopping wave energy devices. In other cases, such as point absorber wave energy devices, the mooring system must leave the floating structure to move “freely” at the wave frequency in order to maximise energy production. In both cases, the slow and large horizontal motion of the floating structure should be restrained because a) the power cable, exporting energy, should not become tensioned, and b) in an array configuration, collisions must be avoided between devices.

This paper presents a methodology developed to evaluate the *relative* risk of marine megafauna entanglement with different mooring systems, focussing on the physical

characteristics of mooring lines that will influence this risk. It is not intended to be a quantitative assessment of risk; this is unfeasible given the scarcity of data available. However, it provides a tool that will enable developers to assess whether their proposed mooring configurations will pose a higher or lower entanglement risk to marine life than alternative systems, and this can then be highlighted in the EIA with appropriate monitoring programmes proposed to mitigate any risk if required. The general methodology, using the hydrodynamic modelling software OrcaFlex, is described in Section 2, with the detailed physical parameters and their specific mode of assessment presented in Section 3. Results are presented for each of the physical parameters, and combined in order to assess the overall relative risk of a particular mooring configuration in Section 4, followed by a discussion of these results and their implication for the industry in Section 5.

2. Modelling methodology

2.1. OrcaFlex model

This investigation utilises OrcaFlex, a 3D time-domain finite element method (FEM) modelling program, to predict the response of the various mooring configurations to wave loading. OrcaFlex is one of the leading software packages for the dynamic analyses of mooring systems and is well validated for this purpose (e.g. [10]). It is widely used in the wave energy sector, both in device development ([11-12]), and in specific wave energy moorings research ([13-14]). Applications also exist for floating wind turbines, for example, a specific coupling module, FASTlink, has been developed in OrcaFlex to integrate the aerodynamic loads, the turbine control system and the flexure of the turbine [15].

2.2. Numerical set-up

Within the model, each mooring line is divided into segments with visco-elastic behaviour, connected by nodes with a given mass (Figure 1). OrcaFlex models are built using a combination of components such as buoys or lines, and environmental conditions (wave, wind or current) are provided as model input.

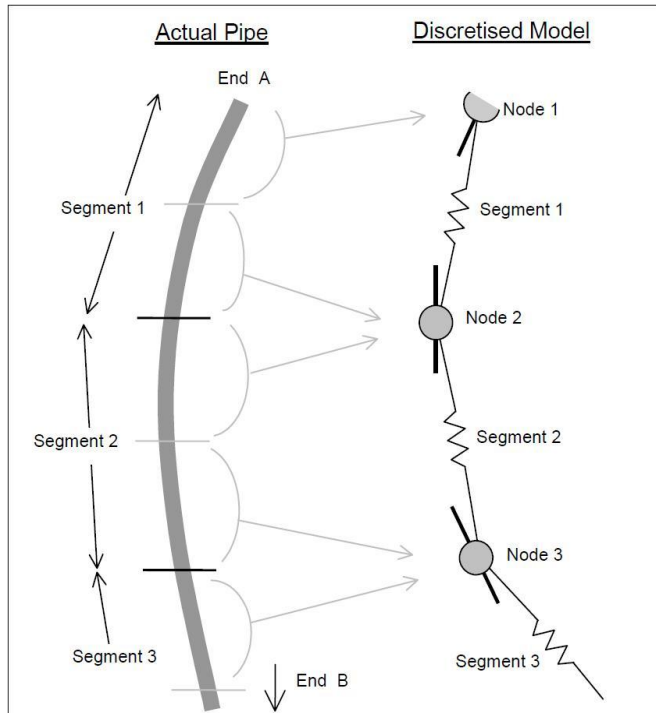


Figure 1. Representation of lines using a finite element model in OrcaFlex [16]. Reproduced with the kind permission of Orcina.

The environmental conditions used in this study are intended to be typical of an ORE installation location. Environmental conditions for the Wave Hub offshore test site in the South West UK have been taken as a reference for this paper. The water depth at the Wave Hub site is approximately 50 m, and OrcaFlex calculations have been run for this water depth.

According to van Nieuwkoop et al. [17]), the 100-year return period significant wave height H_S at Wave Hub is estimated at 9.6 m, and the corresponding wave energy period $T_{m-1,0}$ can be estimated at approximately 12 s according to the provided scatter diagram. The relationship between $T_{m-1,0}$ and the mean zero up-crossing period T_Z is : a) for a Bretschneider spectrum, $T_{m-1,0} = 1.206 T_Z$ and b) for a Jonswap spectrum with $\gamma = 3.3$, $T_{m-1,0} = 1.18 T_Z$ [18]. This means that at Wave Hub, the 100-year return period mean zero up-crossing period T_Z is approximately 10 s. Based on these results, the mooring configurations in this study have been designed for an extreme sea state with a significant wave height $H_S = 10$ m and a mean period $T_Z = 10$ s.

Operational sea states, i.e. the conditions likely to be encountered by the device as part of its normal operation, are defined as regular waves with height H below 10 m and period T below 10 s. Regular waves were used in preference to irregular sea states to observe behaviour at a given frequency and wave steepness, and to reduce the computation time. To limit the number of calculations, only sea states with H of 1, 5 and 10 m are assessed. The wave periods that are too short for a particular wave height, leading to breaking, are not analysed. The regular wave parameters used to analyse operational sea states are summarised in Table 1.

Currents and wind are not considered in this study for simplification, as the intention is to focus only on the main loading forces with the potential to affect entanglement, i.e. those due to wave action.

Table 1. Extreme and operational sea states used in this study

| Extreme sea state | | Operational sea states | |
|-------------------|-----------|------------------------|---------|
| H_S (m) | T_Z (s) | H (m) | T (s) |
| 10 | 10 | 1 | 3-10 |
| | | 5 | 6-10 |
| | | 10 | 7-10 |

The floating structure used for this study is intended to be representative of an ORE device. In order to estimate the typical dimensions of a ORE device, the properties of several existing ORE devices (Table 2) were examined. Based on these properties, the floating structure chosen for analysis is a cylinder with a diameter of 15 m, a height of 10 m, a draft of 8 m (without moorings) and a weight of 1449.1 tonnes. The system extracting energy was not modelled in order to simplify the simulation.

Table 2. Example of dimensions of full-scale floating offshore renewable energy devices

| Device (Company) | Type | Shape | Length (m) | Height (m) | Weight (tonnes) | Draft (m) | Reference |
|---------------------------------------|---|------------------------|-------------------|-------------------|------------------------|------------------|------------------|
| Pelamis P2 (Pelamis Wave Power) | Wave energy: Attenuator | Horizontal cylinders | 180 | 4 | 1350 | | [19] |
| Ocean Energy Buoy (Ocean Energy Ltd) | Wave energy: Oscillating water column | Cuboid | 24 | | 1800 | | [20][21] |
| Bolt 2 LifeSaver (Fred. Olsen) | Wave energy: Point absorber | Square toroid | 16 | 1 | 55 | | [22] |
| CETO (Carnegie Wave Energy Limited) | Wave energy: Point absorber | Vertical cylinder | 11 | | 200 | | [20][23] |
| OPT Mark 3 (Ocean Power Technologies) | Wave energy: Point absorber | Vertical cylinders | 11 | 43.5 | 180 | 32 | [24] |
| Langlee (Langlee Wave Power) | Wave energy: Oscillating wave surge converter | Square frame and flaps | | | 1600 | | [20] |
| Penguin (Wello Oy) | Wave energy: Kinetic energy absorber | Boat hull shape | 30 | 9 | 1600 | 7 | [25] |
| Hywind (Statoil) | Floating wind energy | Vertical cylinder | 6 at water line | | | 10 | [26] |
| WindFloat (Principle Power, Inc) | Floating wind energy | Triangular frame | | | | <20 | [27] |
| BlueTEC (Bluewater) | Floating tidal energy | Horizontal cross | 24 x 40 | | | | [28] |

ORE mooring system configurations are based on traditional mooring configurations. Harris et al. [9] highlight that the most suitable moorings for wave energy devices are single or multi-catenary moorings, catenary anchor leg moorings (CALMs) or single anchor leg moorings (SALMs). Floating wind designs can use tension leg platforms (TLPs), a spar buoy, or a barge [15]. Catenary or taut mooring lines typically connect these platforms to the seabed.

Fitzgerald and Bergdahl [14] investigated catenary moorings and found that the addition of a surface buoy or of a clump weight in the mooring line may improve its performance because it absorbs the motion of the floating structure and consequently reduces the excitation of the mooring cable. Johanning and Smith [12] investigated two catenary configurations using a) chains only, b) chains and nylon ropes and c) one S-shape configurations using nylon ropes only and compared the different mooring behaviours with load-excursion diagrams. They observed that the stiffer configuration (a) experienced higher mooring loads than the more compliant ones (b-c).

Four mooring system configurations have been chosen for this study. The mooring systems used for this study have three equally spread mooring lines attached at the mean water level of the floating structure. In the numerical model, the waves were equally spread between the two front mooring lines, and were aligned with the backward line. The four mooring configurations are described below and illustrated in Figure 2:

- Catenary mooring configuration (Figure 2a)

Mooring lines are connected to the floating structure, freely hanging in the water column and lying on the seabed, applying horizontal loads on the anchor. The part of the mooring lying on the seabed provides the restoring forces with its weight when lifted as shown in Figure 3, which keep the floating structure around its equilibrium position.

This configuration is assessed with different materials: chains only, chains and nylon ropes, and chains and polyester ropes. The aim of using synthetic fibre ropes is to reduce the weight of the mooring on the floating structure and to damp mooring loads with the elasticity of such materials. For the same diameter, Nylon ropes are generally more elastic than polyester ropes. Fibre ropes do not resist abrasion well and should avoid contact with the seabed, which is why they are used only in the water column.

- Taut mooring configuration (Figure 2b)

Mooring lines are connected to the floating structure and are tightly attached to their anchor, forming an angle between the seabed and the mooring line. The taut configuration requires a large pre-tension to avoid the mooring lines becoming slack in wave troughs or at low tide. If a mooring line becomes slack, extreme snap loads may occur when the mooring line becomes re-tensioned. The restoring forces are provided directly by the internal stiffness of the mooring line, as shown in Figure 3.

- Catenary mooring configuration with accessory buoys (Figure 2c)

This configuration is similar to the catenary mooring configuration, but a small accessory buoy is added at the top of each catenary line, and a connecting line is added between this accessory buoy and the floating structure. This aims to reduce the weight of the mooring line on the floating structure and to reduce the mooring loads by smoothing the excitation at the top end of the mooring line. However, with this configuration, the excursion of the floating structure – its maximum surge motion - is more difficult to control.

- Taut mooring configuration with accessory buoys (Figure 2d)

This configuration is similar to the taut mooring configuration, but a small accessory buoy is added at the top of the taut line, and a connecting line is added between this accessory buoy

and the floating structure. The reasoning is the same as for the catenary mooring with accessory buoys, but the same challenges are also present. Other mooring configurations are possible for ORE devices, for example configurations using accessory clump weights. The same methodology can be applied to these other configurations; this paper focuses more on the methodology than on particular mooring arrangements.

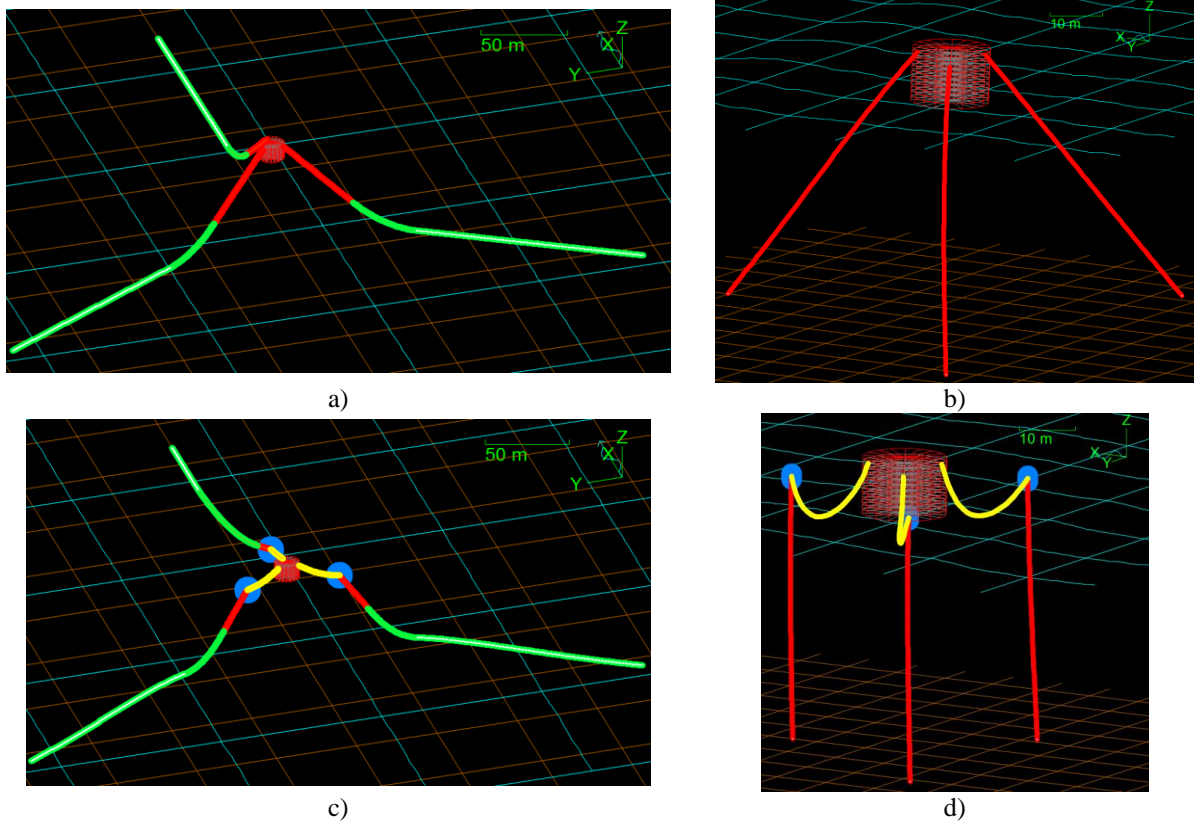


Figure 2. Mooring configurations: a) Catenary mooring configuration with the top lines being chains or synthetic ropes, b) Taut mooring configuration, c) Catenary mooring configuration with accessory buoys, d) Taut mooring configuration with accessory buoys

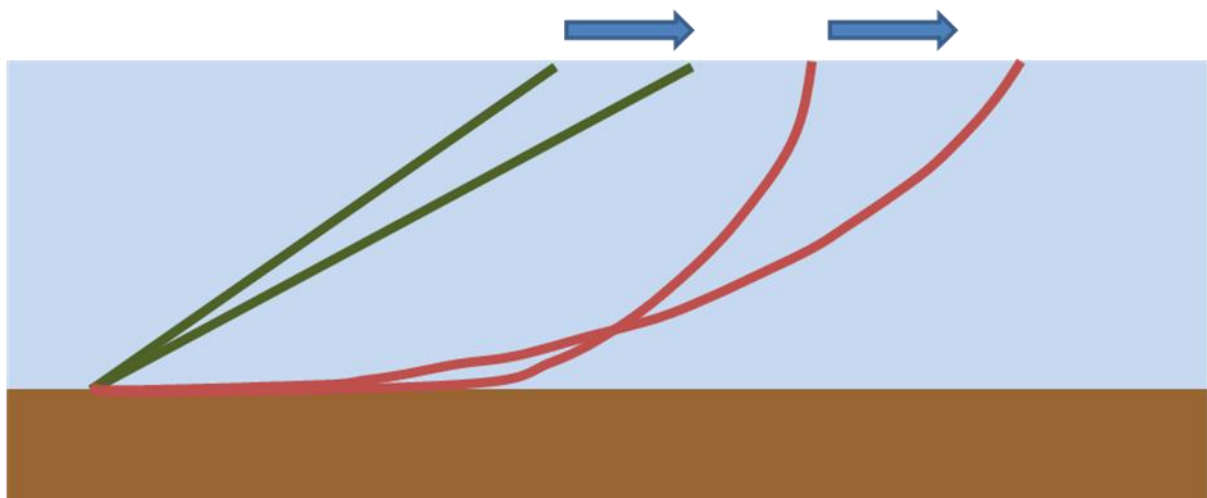


Figure 3. Change in the shape of a taut (left) and catenary (right) mooring lines due to surge of the floating structure

A preliminary assessment was carried out with the extreme sea state ($H_S = 10$ m and $T_Z = 10$ s) for each mooring configuration to assess the order of magnitude of the maximum mooring loads and ensure that the mooring strength is correctly defined. This means that the maximum load multiplied by a factor of safety is below the minimum breaking load (MBL) of the weakest element of the mooring system. This leads to mooring system materials and dimensions as described in Table 3. The material properties (displacement, MBL, axial stiffness and mass per unit length) were taken as calculated by OrcaFlex. It should be noted that for a more accurate design, the manufacturer specific properties should be considered. A more detailed analysis would also be required to design these mooring systems for a real device.

Table 3. Mooring properties for this study. All chains are Grade 3 and studlink.

| | 1) Catenary | | | 2) Taut | 3) Catenary & accessory buoy | 4) Taut & accessory buoy | |
|-------------------------|---|------------------|-----------------------|---------------------------|------------------------------|--------------------------|-------------|
| Top | Material | a) Chains | b) Nylon ropes | c) Polyester ropes | Nylon ropes | Nylon ropes | Nylon ropes |
| | Length (m) | 57.5 | 52.8 | 54.25 | 64.8 | 28.5 | 46.6 |
| | Diameter (m) | 0.045 | 0.140 | 0.200 | 0.19 | 0.140 | 0.19 |
| | Displacement (te/m) ¹ | 0.0058 | 0.011 | 0.024 | 0.021 | 0.011 | 0.0084 |
| | MBL² (kN) | 1603 | 2731 | 6818 | 5030 | 2731 | 2007 |
| | Axial stiffness (kN) | 204525 | 2313 | 43600 | 4260 | 2313 | 4260 |
| | Mass per unit length (te/m) | 0.044 | 0.013 | 0.032 | 0.023 | 0.013 | 0.0093 |
| | Distance (m) between nodes for swept volume assessment | 10 | 10 | 10 | 2.6 | 4.5 | 2.3 |
| Bottom | Material | Chains | Chains | Chains | - | Chains | - |
| | Length (m) | 175 | 175 | 175 | - | 175 | - |
| | Diameter (m) | 0.064 | 0.064 | 0.064 | - | 0.064 | - |
| | Displacement (te/m) | 0.012 | 0.012 | 0.012 | - | 0.012 | - |
| | MBL (kN) | 3121 | 3121 | 3121 | - | 3121 | - |
| | Axial stiffness (kN) | 413696 | 413696 | 413696 | - | 413696 | - |
| | Mass per unit length (te/m) | 0.090 | 0.090 | 0.090 | - | 0.090 | - |
| | Distance (m) between nodes for swept volume assessment | 12.5 | 12.5 | 12.5 | - | 12.5 | - |
| Connector | Material | - | - | - | - | Chains | Chains |
| | Length (m) | - | - | - | - | 25 | 25 |
| | Diameter (m) | - | - | - | - | 0.05 | 0.04 |
| | Displacement (te/m) | - | - | - | - | 0.0072 | 0.0046 |
| | MBL (kN) | - | - | - | - | 1960 | 1279 |
| | Axial stiffness (kN) | - | - | - | - | 252500 | 161600 |
| | Mass per unit length (te/m) | - | - | - | - | 0.055 | 0.035 |
| | Distance (m) between nodes for swept volume assessment | - | - | - | - | 1.25 | 1.25 |
| Other properties | Accessory buoy volume (m³) | - | - | - | - | 3 | 5.3 |
| | Accessory buoy mass (te) | - | - | - | - | 0.05 | 0.05 |
| | Distance centre floating structure-anchor (m) | 220 | 220 | 220 | 50 | 220 | 50 |
| | MBL mooring (kN) | 1603 | 2731 | 3121 | 5030 | 1960 | 1279 |
| | Pre-tension (kN) | 50 | 50 | 50 | 1000 | 50 | 50 |
| | Pre-tension/MBL % | 3.1% | 1.8% | 1.6% | 19.9% | 2.6% | 3.9% |

¹ The displacement is the weight of the volume of water occupied by the mooring line.

² Minimum Breaking Load

3. Parameters relating to entanglement risk

Three key parameters were considered to assess the relative risk of entanglement for the selected mooring systems. These parameters were investigated with the OrcaFlex numerical models described in the previous section. The first parameter evaluates the stiffness of the mooring system using the tension characteristics, because slack moorings are more likely to cause entanglement than taut moorings. If an animal comes into contact with a loosely hanging mooring line, the risk of being entangled is higher than with a taut line. The second parameter evaluates the volume of water occupied by the mooring line in a particular sea state. If this volume is high, then it means that the mooring lines are moving significantly, and that the risk of contact between a marine animal and a mooring line is higher. The third parameter assesses the curvature of the mooring line. The higher the potential curvature of a mooring line, the greater the risk, if an animal comes into contact with it, that the line could form a loop around the body of the animal from which it would be unable to extract itself. The three different parametric studies are described below.

3.1. *Tension characteristics*

The tension characteristics were estimated by slowly surging the floating structure forward and backward with no environmental loads (i.e. wave, wind or current forces). The floating structure was moved from a minimum distance of -100m to a maximum distance of +100m in the alignment of the backward line. Mooring loads in the three mooring lines as well as horizontal surge were used to plot the tension characteristics. For comparison purposes, dimensions were removed by dividing the mooring load by the MBL of the mooring system, and the surge position by the water depth.

Johanning and Smith [12] investigated tension characteristics in order to compare different mooring configurations in terms of restoring forces for a range of excursions of a floating structure. It was found that the increase in tension is non-linear relative to the excursion for a catenary mooring for a moderate excursion while the chains are lifted, but is linear for a taut configuration because of the internal line stretching. A simplified version of these results is presented in Figure 4.

For the mooring configurations considered in this study, the tension characteristics curve is expected to be asymmetrical. When the floating structure is moving in one direction, two lines are tensioned and the other one is slackened, while when the floating structure is moving in the other direction, only one line is tensioned and two are slackened.

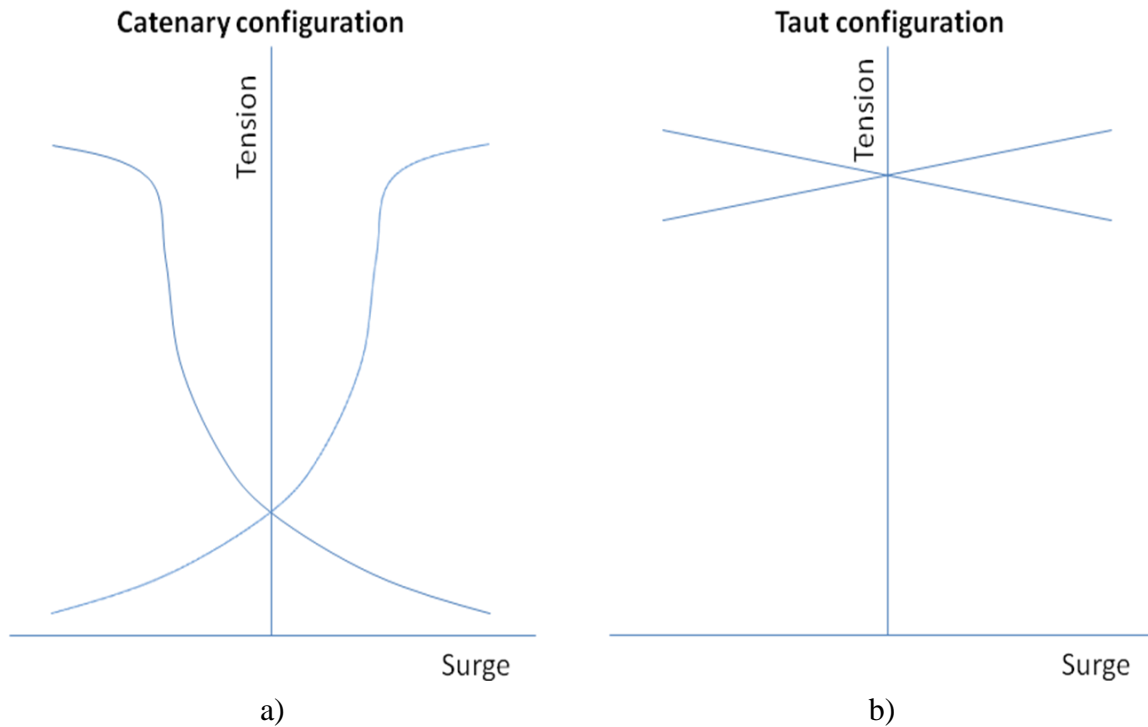


Figure 4. Examples of tension characteristics for different a) catenary and b) taut mooring configurations with two opposite lines (adapted from Johannig and Smith [12]).

3.2. Mooring line swept volume ratio

The volume of water swept by the mooring lines was estimated for the different sea states described in Table 1. An example of swept volume is shown in Figure 5a, with the swept volume highlighted in grey. In order to estimate this swept volume, the methodology described below was developed and applied. For each simulation, the time series of the physical position of 10 alternate nodes from the top of the mooring line was recorded with a timestep of 0.1 s. The distance between nodes for these simulations is dependent on the mooring configuration and is given in Table 3. However, this method ensured that for all configurations, the length of the moving part of the mooring line through the water column was considered. This limited resolution was aimed at reducing the computational time and the size of OrcaFlex output files. Using these time series, the process to estimate the swept volume ratio was the following:

- a) A large rectangular cuboid, containing the maximum and minimum positions of all nodes was drawn and then divided into 200 x 200 x 200 small rectangular cuboids. The size of these small cuboids varied between simulations because the maximum and minimum node positions were dependent on the mooring configuration and sea states. For example, for $H = 1$ m and $T = 3$ s, for the taut configuration, the size of a cuboid was 0.36 m x 0.41 m x 0.25 m and for the catenary configuration the size of a cuboid was 1.5 m x 1.7 m x 0.27 m.
- b) Each small cuboid was marked as occupied if the mooring line passed inside it at any time during the simulation. The volume of all the occupied small cuboids was summed to obtain the total occupied volume. This total occupied volume was then divided by the volume of the

mooring lines for comparison purposes to calculate a swept volume ratio. The volume of the mooring lines was estimated using the displacement of the mooring lines, i.e. the weight of the water occupying the same volume than the mooring line.

Figure 5b shows a simplified low definition two-dimensional example of this process.

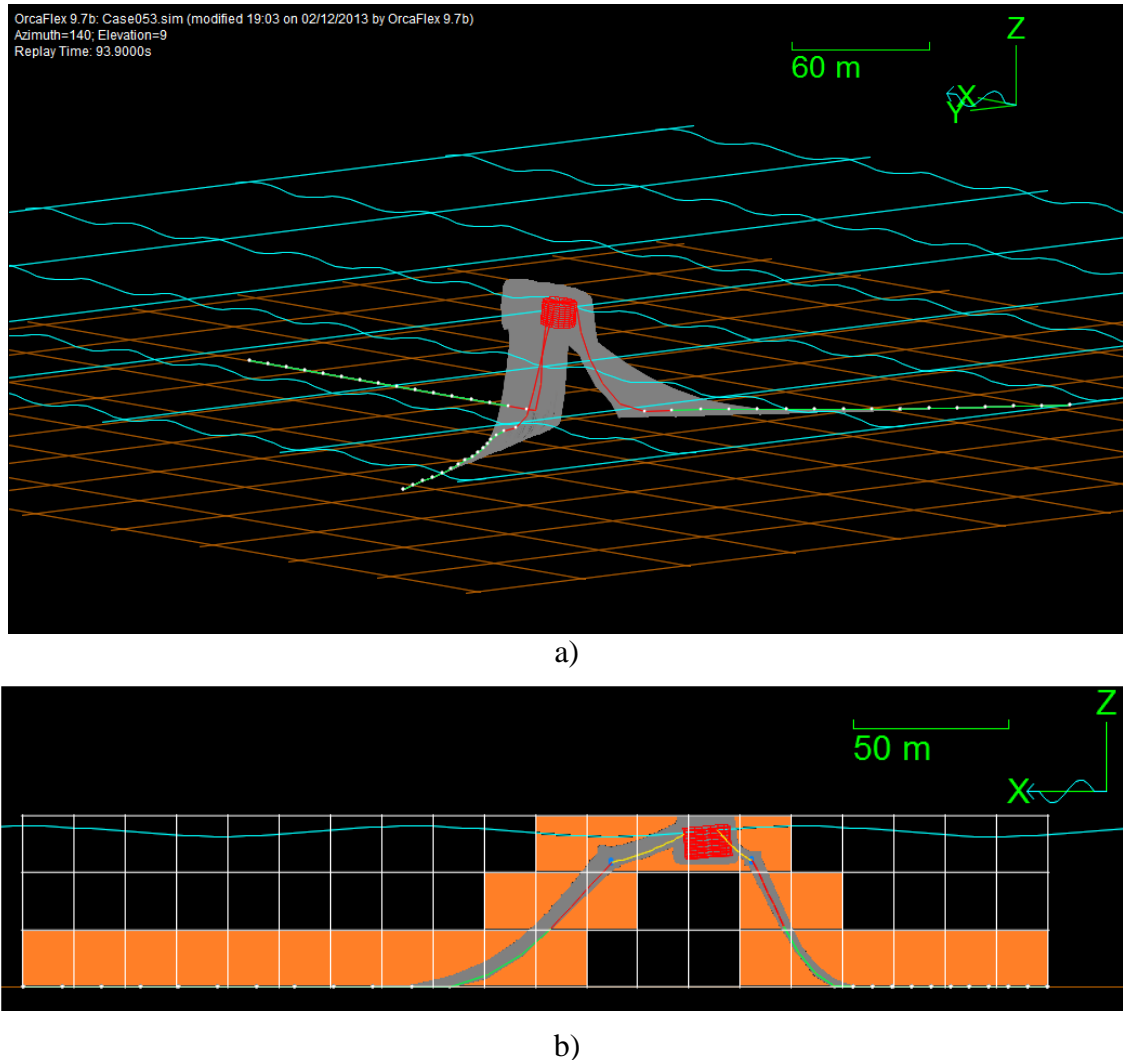


Figure 5. Swept volume assessment. a) example of swept volume in grey, b) simplified process in 2D with low definition to estimate the swept volume. Orange cells are occupied cells

3.3. Mooring line curvature

The curvature was directly estimated by OrcaFlex as the angle change at a node divided by the segment length (0.5 m for all mooring configurations in this curvature study). The curvature is then expressed in degrees per metre. The curvature was considered only for the nodes in the water column, i.e. those not lying on the seabed, and for the main mooring line (not the connectors). Examples of curvature values are given in Figure 6. For the catenary configuration (Figure 6a), the curvature is higher near the touchdown point (the point of contact between the mooring line and the seabed) because the line is forced to become

horizontal on the seabed. The curvature is also high at the top end of the mooring line, because of its dynamic behaviour. The curvature is relatively small in the water column. For the taut configuration (Figure 6b), the curvature is low all along the mooring line.

For this study, the curvature of the backwards line was observed for the maximum excursion of the floating structure in a regular sea state with $H = 1$ m and $T = 6$ s. The backwards line was chosen because this line is the most likely to become slack and to display high curvature values because of the drifted position of the floating structure.

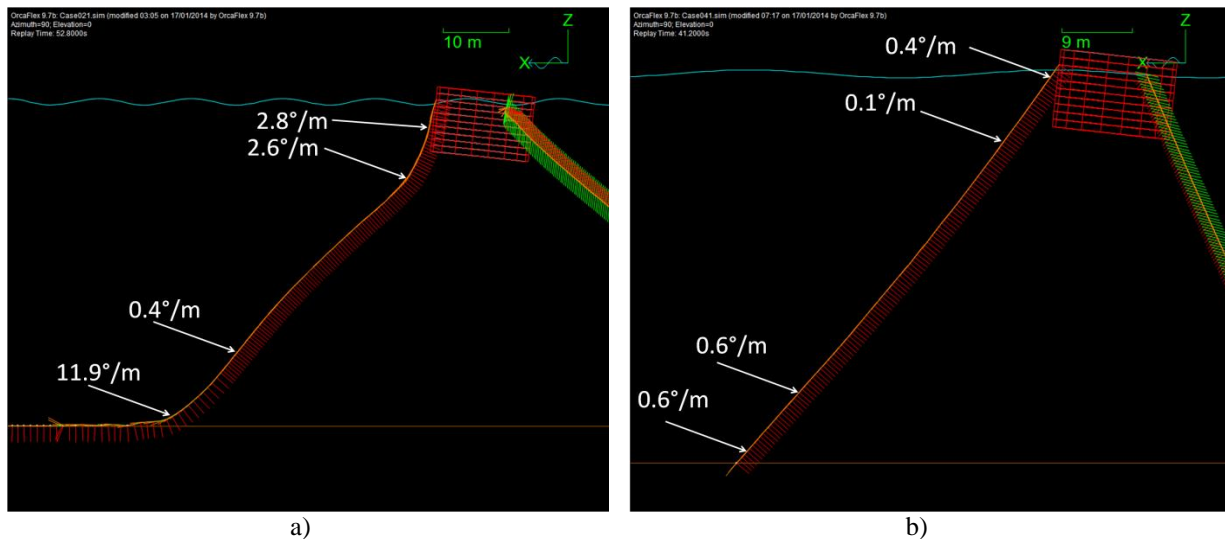


Figure 6. Example of curvature calculation in OrcaFlex a) for a catenary configuration and b) for a taut configuration

4. Results

For each parameter affecting entanglement and for each mooring configuration, the relative risk of entanglement was assessed based on the results of the parametric studies. This enabled a risk 'score' to be assigned to each mooring configurations. Risk scores ranged from 1 to 3, with 1 representing a lower risk and 3 a higher risk. It is important to emphasise that this is a relative risk score, comparing the different mooring configurations, and is not intended to quantify the actual risk. Results were then summarised to give an overall relative risk of entanglement for each mooring configuration. The aim is to classify the different mooring configurations in terms of entanglement in order to assess which configuration has a relatively higher risk of entanglement.

4.1. Tension characteristics

Tension characteristics for the different mooring arrangements are plotted in Figure 7. As expected, the tension characteristics are asymmetrical. Results indicate a low tension to MBL slope for small to medium surge for the catenary moorings (Figure 7a-c), allowing a considerable flexibility in the mooring. The use of nylon ropes (Figure 7b) even enhances this flexibility because of the elasticity and low weight of nylon ropes. Because the polyester line has a considerably higher axial stiffness and a higher weight (Table 3) than the nylon lines, the catenary mooring using polyester ropes (Figure 7c) behaves very similarly to the catenary

mooring using chains only (Figure 7a) in terms of tension characteristics. The taut mooring system shows a high tension to MBL slope for all ranges of surge (Figure 7d), meaning that this mooring system provides large restoring forces for any range of excursion. The addition of accessory buoys to the catenary configurations (Figure 7e) makes the configuration slightly more flexible, while the addition to the taut configuration (Figure 7f) makes it largely more flexible, with a near-constant tension to MBL ratio across the surge range.

The physical meaning of these results can be observed in Figure 8, with the different mooring arrangements for a given excursion. The length of chains lifted is different for each catenary configuration (Figure 8a-c), leading to different tensions for the same excursion. A mooring line is stretched in the taut configuration (Figure 8d). The accessory buoys and connectors are accommodating a portion of the excursion (Figure 8e-f).

These results mean that with a taut arrangement with accessory buoys, the floating structure can move freely for the range of excursion investigated, while for the taut configuration, the floating structure motions are restrained. The other configurations provide a range of restoring forces between these two extreme conditions.

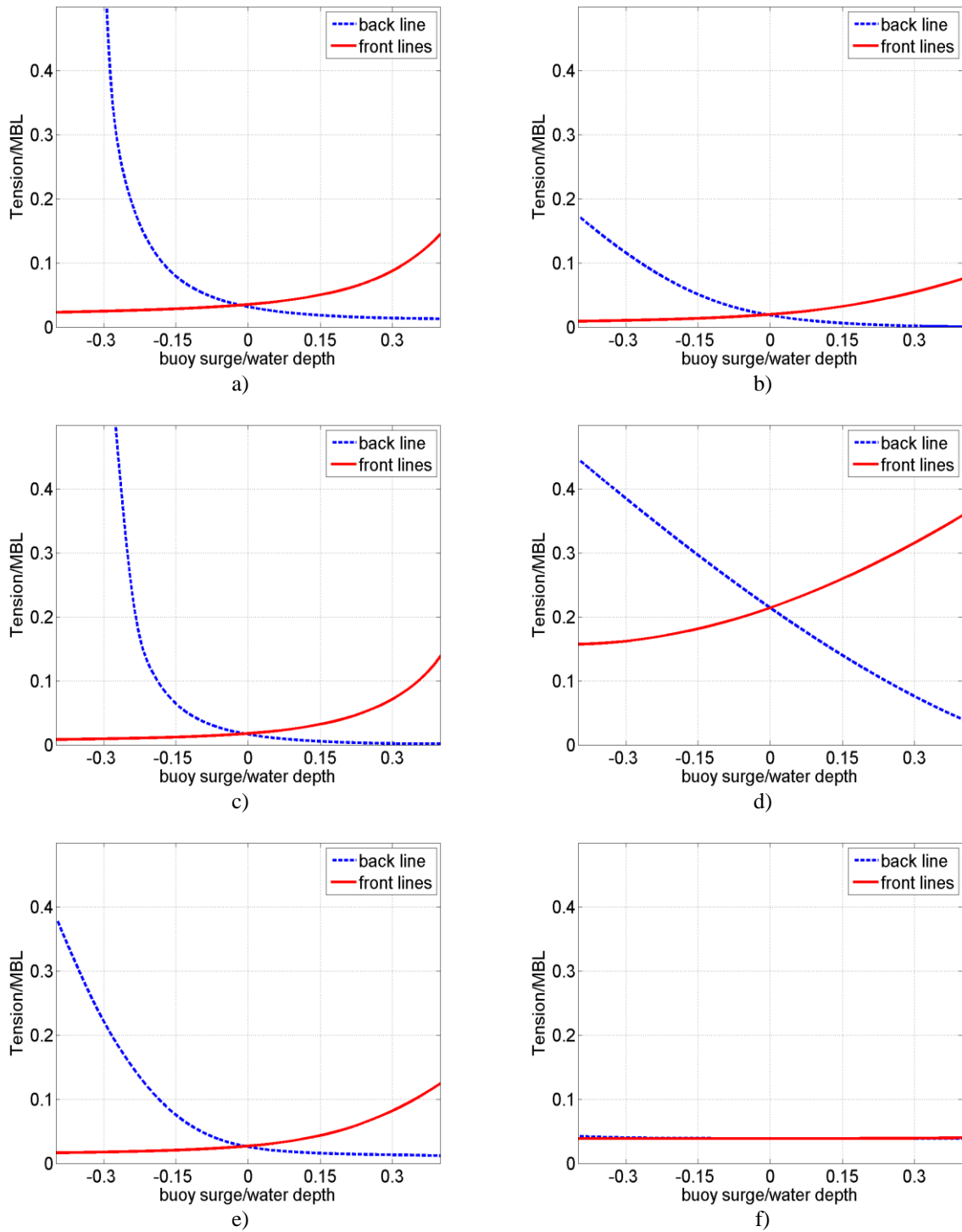


Figure 7. Tension characteristics for the different mooring arrangements: a) Catenary, b) Catenary with chains and nylon ropes, c) Catenary with chains and polyester ropes, d) Taut, e) Catenary with accessory buoys, f) Taut with accessory buoys

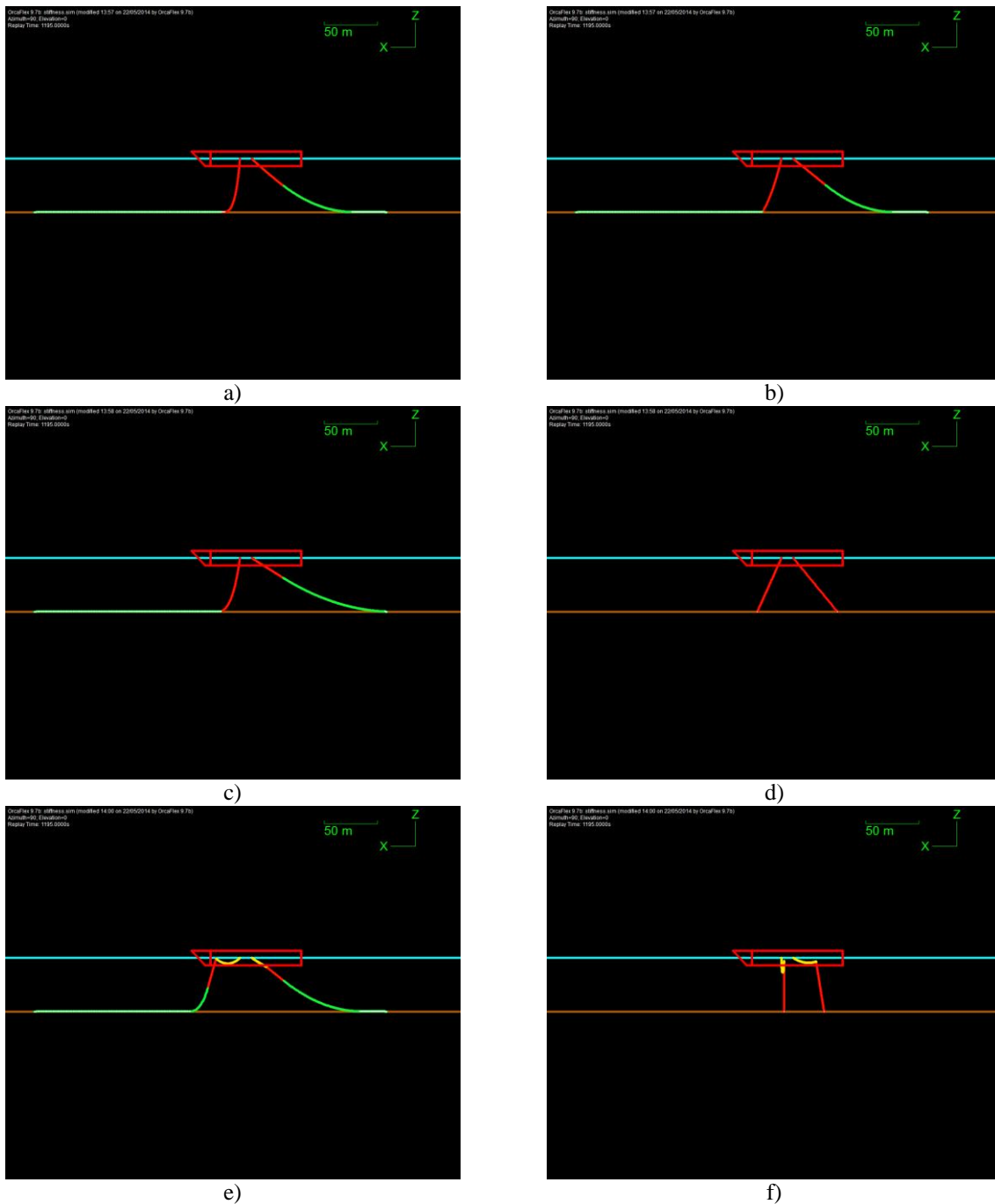


Figure 8. Example for an excursion of 20m of the layout of the different mooring configurations: a) Catenary, b) Catenary with chains and nylon ropes, c) Catenary with chains and polyester ropes, d) Taut, e) Catenary with accessory buoys, f) Taut with accessory buoys

The risk score for each mooring configuration was established through a 3-step process:

1. The plots in Figure 7 are horizontally and vertically divided into cells, and the axes are correspondingly divided into surge and tension scores, as shown in the example in Figure 9. Each cell can therefore be associated with a risk, which is its surge score multiplied by its tension score. If this number is below or equal to 5, the risk is relatively low; if this number is between 6 and 10 then the risk is medium; and if the risk is equal to or over 11 then the risk is relatively high.

2. The number of low, medium and high risks cells intersected by the tension characteristics curve are counted and input in Table 4. A weighted average surge/tension score is calculated. A score of 1 is associated with each low-risk cell intersected, two for each medium-risk cell and 3 for each high-risk cell. The final surge/tension score is calculated by dividing the summed total by the total number of intersected cells.

3. If the final surge/tension score is below 1.75, the mooring system is assumed to be low risk and given a risk score of 1 for its tension characteristics. A surge/tension score between 1.75 and 2 is given a risk score of 2, and for surge/tension scores greater than 2, a risk score of 3 is allocated, indicating that there is a relatively higher risk of entanglement for that mooring configuration. The final results are summarised in Table 4.

Results indicate that when considering only the tension characteristics, the relative risk of entanglement is higher for the catenary with chains and nylon ropes, the catenary with accessory buoys and the taut with accessory buoys arrangement. The lowest risk is seen for the taut configuration.

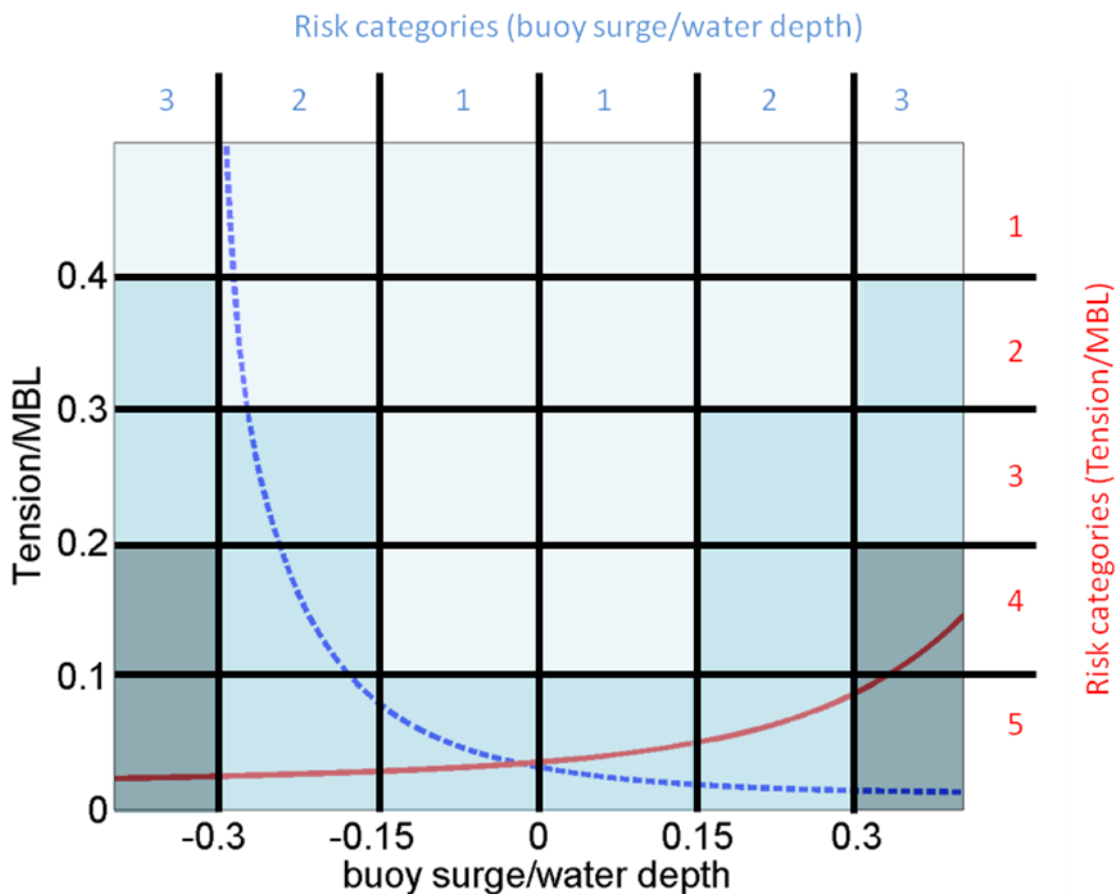


Figure 9. Example of parameterised risk pattern for the tension characteristics. The surge and tension scores are multiplied. Light colour indicates relatively low risk while darker colours indicate increasing risk.

Table 4. Summary of risk assessment for the tension characteristics

| | Number of low risk cells | Number of moderate risk cells | Number of high risk cells | Total number of cells | Average surge/tension score (AS) | Final tension risk parameter score |
|--|--------------------------|-------------------------------|---------------------------|-----------------------|----------------------------------|--|
| Example | x | y | z | x+y+z | $\frac{x + 2y + 3z}{x + y + z}$ | =1, AS<1.75 =2, 1.75≤AS<2 =3, 2≤AS |
| Catenary & chains | 6 | 6 | 3 | 15 | 1.80 | 2 |
| Catenary & chains & nylon ropes | 4 | 5 | 4 | 13 | 2.00 | 3 |
| Catenary & chains & polyester ropes | 6 | 6 | 4 | 16 | 1.88 | 2 |
| Taut | 9 | 6 | 2 | 17 | 1.59 | 1 |
| Catenary & accessory buoys | 4 | 8 | 4 | 16 | 2.00 | 3 |
| Taut & accessory buoys | 4 | 4 | 4 | 12 | 2.00 | 3 |

4.2. Swept volume

The swept volume ratios are plotted in Figure 10 for the different sea states and the six mooring configurations considered in this study. For $H = 1$ m and $H = 5$ m, the swept volume ratios tend to decrease when the wave period increases, because the steepness of the wave decreases. However, this is not the case for $H = 10$ m because the sea states are highly energetic.

Catenary moorings, with (Figure 10e) or without (Figure 10a-c) accessory buoys, have large swept volume ratios and exhibit similar behaviours. In contrast, the taut configurations, with (Figure 10f) and without (Figure 10d) accessory buoys, have significantly lower swept volume ratios, especially with the accessory buoys.

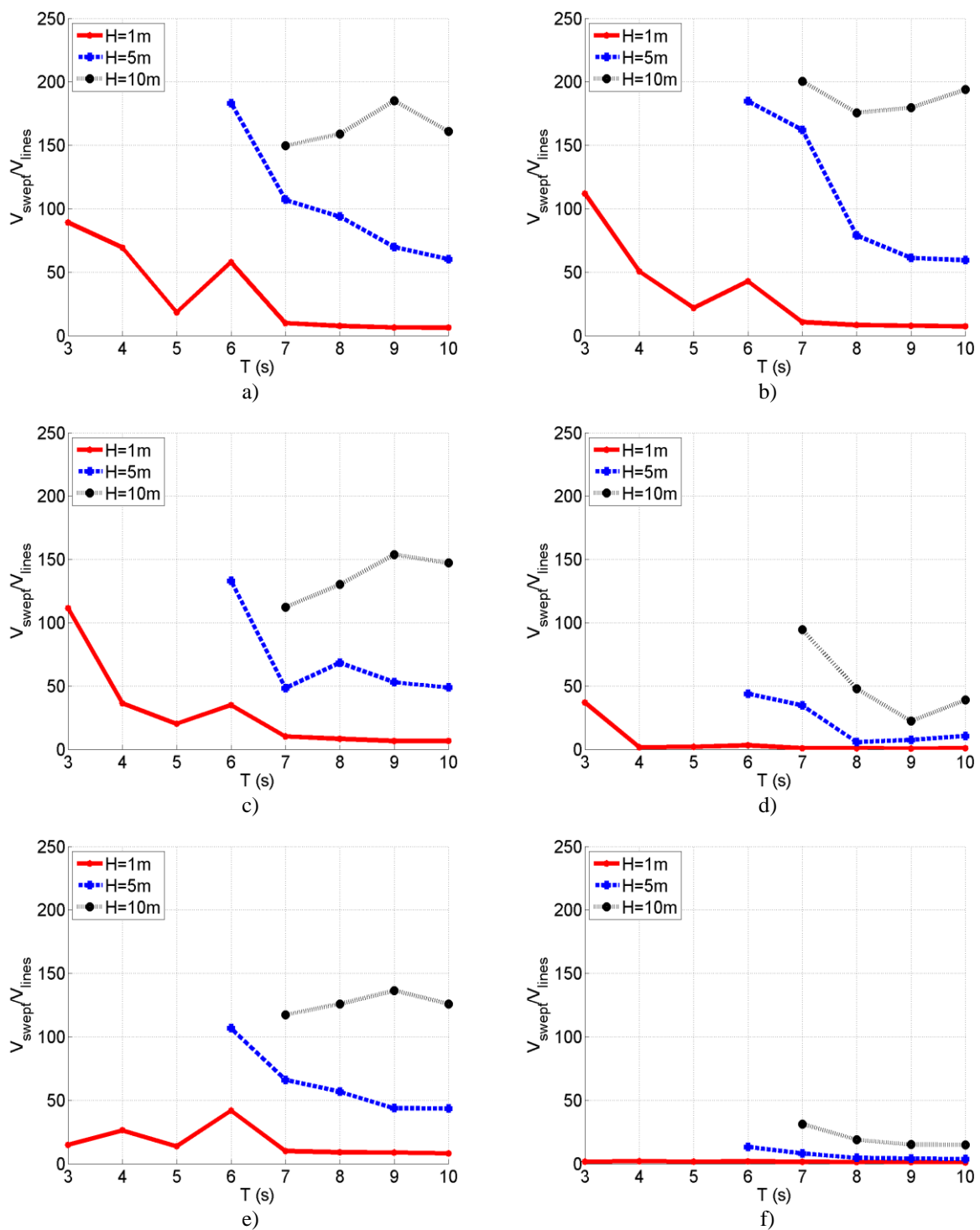


Figure 10. Swept volume ratio (V_{swept}/V_{lines}) occupied by the different mooring configurations at different sea states: a) Catenary, b) Catenary with chains and nylon ropes, c) Catenary with chains and polyester ropes, d) Taut, e) Catenary with accessory buoys, f) Taut with accessory buoys

Figure 11 gives more insight into the mooring line contributions to the swept volume ratio. For the catenary configurations (Figure 11a-c and e), the mooring lines are significantly sweeping and the swept volume V_{swept} is then high. However, the line volume V_{lines} is also

relatively high because of the long length of the mooring lines and this minimises the swept volume ratio. For the taut configurations (Figure 11d and f), the swept volume V_{swept} is low but the line volume V_{lines} is also relatively low because of the short length of the mooring lines and this increases the swept volume ratio. The line volume V_{lines} is higher for the configuration with accessory buoys which explains why the swept volume ratio is lower with the accessory buoys than without.

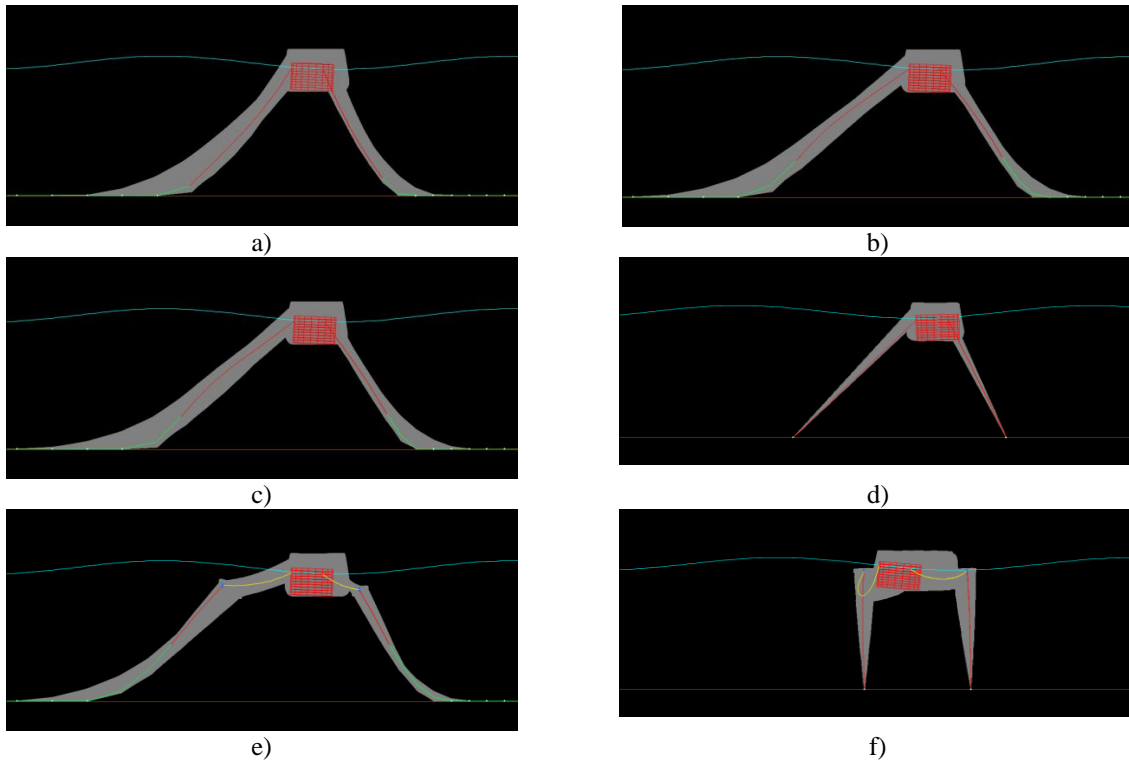


Figure 11. Example for $H = 5$ m and $T = 9$ s of trails showing the swept volume occupied by the different mooring configurations: a) Catenary, b) Catenary with chains and nylon ropes, c) Catenary with chains and polyester ropes, d) Taut, e) Catenary with accessory buoys, f) Taut with accessory buoys

In order to provide a risk score, graphs in Figure 10 are horizontally and vertically divided into cells, with each assigned an indicative score defining the relative entanglement risk (Figure 12): for a swept volume ratio below 100, the score is 1; for a volume ratio between 100 and 200, the score is 2; and for a volume ratio over 200, the score is 3. These numbers are averaged and rounded for the different sea states, giving a final swept volume score (Table 5).

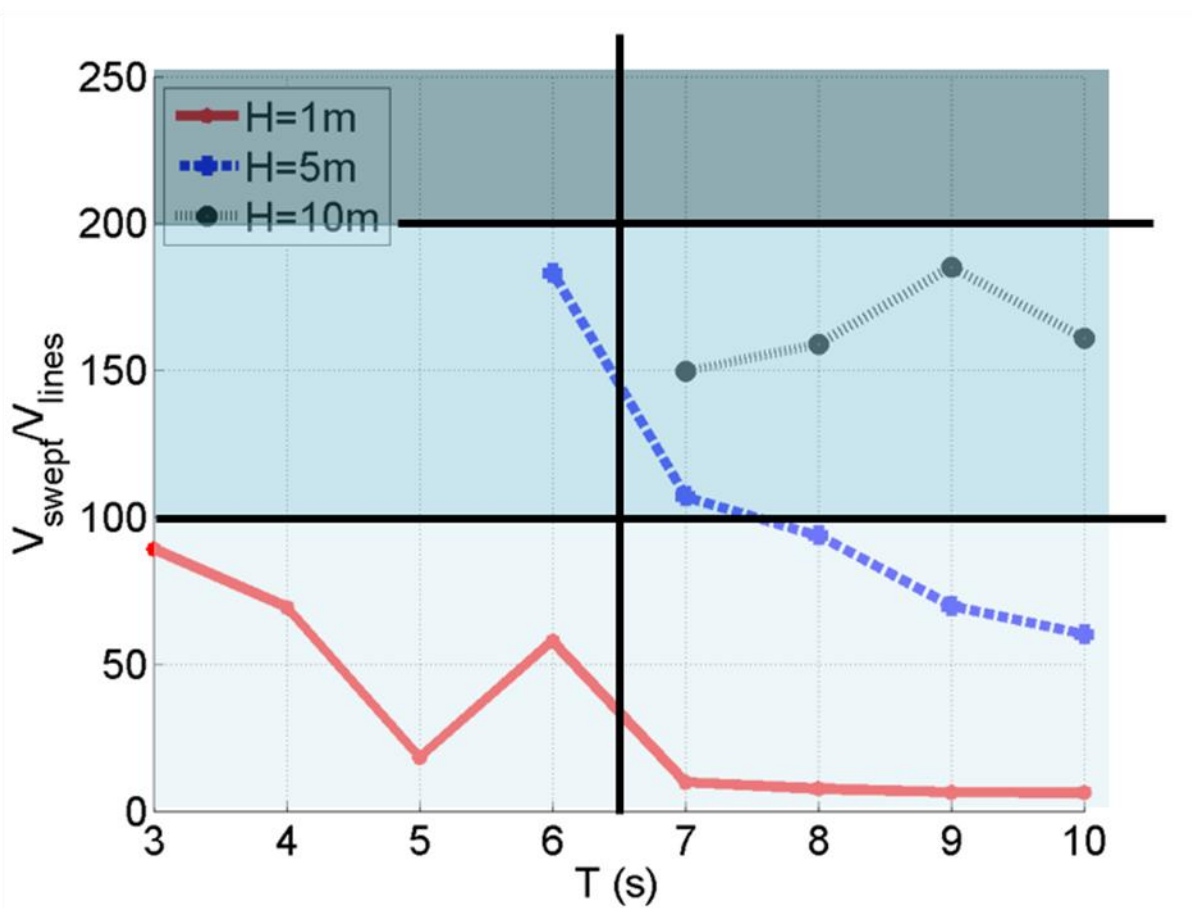


Figure 12. Example of parameterised risk pattern for the swept volume ratio. Light colour indicates relatively low risk while darker colours indicate increasing risk.

| Mooring type | Highest score associated with: | | | | | Average score (AS) across sea states | Final Swept Volume score |
|-----------------------------------|--------------------------------|-------------------|----------|----------|---|--------------------------------------|--------------------------|
| | Wave period T (s) between | Wave height H (m) | | | | | |
| | | 1 | 5 | 10 | | | |
| Example | 3-6 7-10 | x1 x2 | y1 y2 | z1 z2 | $\frac{x1 + y1 + z1 + x2 + y2 + z2}{6}$ | Round(AS) | |
| Catenary chains & nylon ropes | 3-6 7-10 | 1 1 | 2 2 | - 2 | 1.6 | 2 | |
| Catenary chains & polyester ropes | 3-6 7-10 | 2 1 | 2 1 | - 2 | 1.6 | 2 | |
| Taut | 3-6 7-10 | 1 1 | 1 1 | - 1 | 1.0 | 1 | |
| Catenary accessory buoy | 3-6 7-10 | 1 1 | 2 1 | - 2 | 1.4 | 2 | |
| Taut accessory buoy | 3-6 7-10 | 1 1 | 1 1 | - 1 | 1.0 | 1 | |

Table 5. Summary of risk assessment for the swept volume ratio

Results indicate that the relative risk of entanglement relating to the swept volume ratio of the mooring lines is moderate for all catenary configurations, with or without accessory buoys, and low for both taut configurations.

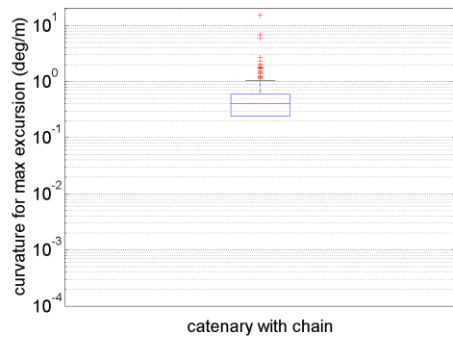
4.3. Curvature

The range of curvature values along the mooring line during its maximum horizontal excursion are plotted in Figure 13. For each box plot, the red central line represents the median value and the edges of the box are the 25th and 75th percentiles. The whisker extends to the most extreme data points not considered outliers, and outliers are plotted individually with red crosses. Due to the logarithmic scale, the lower whisker of the box is not shown.

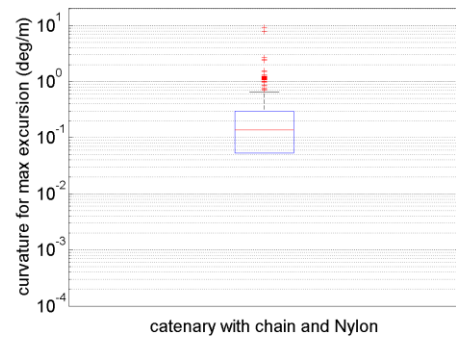
Catenary mooring configurations (Figure 13a-c) have the highest value of curvature because of their low pre-tension and curved shape in the water column. The use of nylon ropes in the catenary line (Figure 13b) produces a decrease in the curvature values. The use of polyester ropes also gives a slightly smaller decrease (Figure 13c). Taut configurations (Figure 13d) have significantly lower values of curvature than any other configurations, although these increase with the addition of accessory buoys (Figure 13f). The catenary configuration with accessory buoys (Figure 13e) has a smaller curvature than the catenary configuration without accessory buoys (Figure 13a).

An understanding of the physical meaning of these curvatures can be obtained from Figure 14 which shows the different mooring configurations at maximum excursion. The left line was the one used for curvature analysis, excluding the connector. Between the different catenary configurations (Figure 14a-c), the touchdown point is at slightly different positions because of the difference in weight of the mooring lines, leading to differences in curvature. For the catenary mooring with chains, the touchdown point of the mooring line is the closest to the buoy; this configuration also shows the highest curvature values, and all curvature values are high. For the taut configuration (Figure 14d), the lines are straight because of their high pre-tension, which explains the small values of curvature. For the catenary configuration with accessory buoys (Figure 14e), the curvature is lower than without accessory buoys, because part of the excursion of the buoy is compensated by the connectors. For the taut configuration using accessory buoys (Figure 14f), the pre-tension is lower in the taut section than in the case without accessory buoys, and this leads to higher values of curvature, with the mooring line being slightly bent.

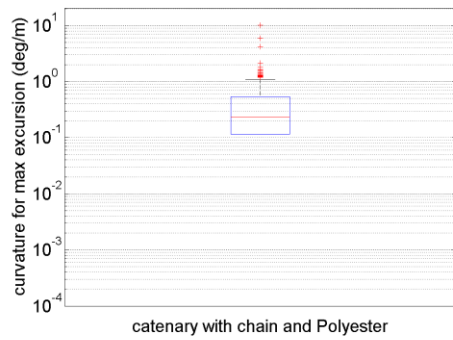
Graphs in Figure 13 are vertically divided into three and assigned indicative scores to enable the assessment of risk, as shown for example in Figure 15. For a median curvature value below 10^{-2} , the score is 1; for a median curvature value below 10^0 , the score is 2; and for a median curvature value over 10^0 , the score is 3. The results are summarised in Table 6.



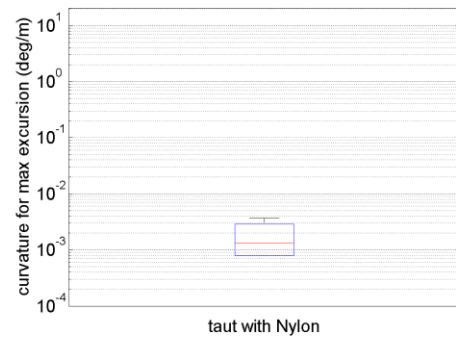
a)



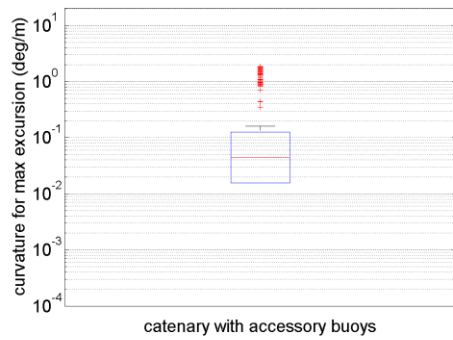
b)



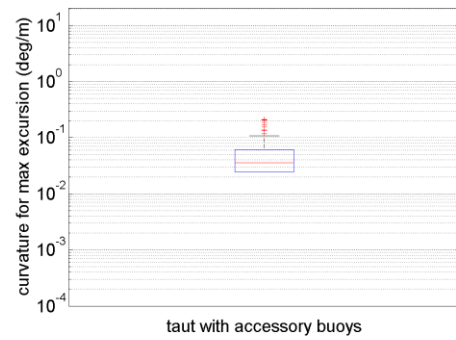
c)



d)



e)



f)

Figure 13. Boxplots of modelled mooring curvatures of the six configurations considered in this report. a) Catenary, b) Catenary with chains and nylon ropes, c) Catenary with chains and polyester ropes, d) Taut, e) Catenary with accessory buoys, f) Taut with accessory buoys



a)



b)



c)



d)



e)



f)

Figure 14. Curvature analysis at the maximum excursion for the different mooring configurations: a) Catenary, b) Catenary with chains and nylon ropes, c) Catenary with chains and polyester ropes, d) Taut, e) Catenary with accessory buoys, f) Taut with accessory buoys



Figure 15. Example of parameterised risk pattern for the curvature. Light colour indicates relatively low risk while darker colours indicate increasing risk.

| Mooring type | Median curvature (degrees per m) at maximum excursion of the buoy | Curvature score |
|-------------------------------------|---|-----------------|
| Catenary & chains | 0.4062 | 2 |
| Catenary & chains & nylon ropes | 0.1364 | 2 |
| Catenary & chains & polyester ropes | 0.2292 | 2 |
| Taut | 0.0013 | 1 |
| Catenary & accessory buoy | 0.0441 | 2 |
| Taut & accessory buoy | 0.0360 | 2 |

Table 6. Summary of risk assessment for the curvature

4.4. Overall relative risk

The entanglement risk based on the three investigated physical characteristics of the mooring is summarised in Table 7 for the different mooring configurations. These results show that the taut configuration is associated with low risks for the three different risk parameters and consequently presents the lowest entanglement risk. The total score is comparable for the other mooring arrangements.

Table 7. Summary of risk assessment for the different mooring parameters

| Mooring type \ risk parameters | Tension characteristics | Swept volume ratio | Curvature | Total score |
|-------------------------------------|-------------------------|--------------------|-----------|-------------|
| Catenary & chains | 2 | 2 | 2 | 6 |
| Catenary & chains & nylon ropes | 3 | 2 | 2 | 7 |
| Catenary & chains & polyester ropes | 2 | 2 | 2 | 6 |
| Taut | 1 | 1 | 1 | 3 |
| Catenary & accessory buoy | 3 | 2 | 2 | 7 |
| Taut & accessory buoy | 3 | 1 | 2 | 6 |

5. Discussion

This paper has presented a method to enable comparison of the relative entanglement risk of different mooring configurations. Results indicate that the taut configuration considered in this study has a significantly lower relative entanglement risk than all the other investigated configurations. The catenary configuration using chains and nylon ropes and the catenary configuration using accessory buoys have the highest relative risk. However, the other catenary configurations, with chains only or with chains and polyester ropes, and the taut configuration with accessory buoys also have high relative entanglement risks.

Although these results are in no way intended to quantify the risk of entanglement, they do indicate that specific features of mooring systems may increase or decrease the risk. This paper gives a method which can be used to compare particular mooring systems but does not mean for example that all taut configurations always have a lower relative entanglement risk.

It should also be highlighted that the risk calculated in this report is a relative risk, and high relative risk does not mean a high and frequent actual risk.

Entanglement could be taken into account from the early design stage of the mooring; furthermore, the parameters required for entanglement assessment are also required for the other technical or financial considerations required for mooring design. A way to integrate entanglement into the early stage of the design system is to include it in EIA reporting process, as suggested by Stefanovich and Fernández Chozas [29] or Equimar [1]. EMEC [30] introduces a list of parameters that developers should provide for the EIA, including entanglement. These parameters encompass the full dimensions of the device, its weight, its draft, the mooring area of coverage, the mooring materials, and the movement of device around mooring. Some of these parameters are required by the methodology proposed in this paper. In order to apply the methodology described in this paper, the following parameters are required:

Moorings

- Mooring layout: number of lines, distance between the centre of the floating structure and the anchor
- Length of each mooring line section
- Line material properties: displacement, mass per unit length, axial stiffness
- If accessory buoys are used: volume, mass

Floating structure

- Hydrodynamics properties: for a small structure, data to apply Morison theory; for a large structure, data to apply the potential radiation-diffraction theory

Environment

- Water depth
- Operational and extreme sea states

These results can be extended to an array of devices or to power cables. However, power cables are less critical than mooring lines. Unlike mooring lines, marine megafauna are likely to be able to break a power cable which has a lower MBL than mooring lines since it is not intended to play any role in keeping a device on station.

The method developed in this paper does not consider derelict fishing gears which can add a potentially significant risk of entanglement, especially in a dense array configuration. If a lost or discarded net, moving freely in the water column with the ocean currents, were to become entangled in one or more mooring lines, the entanglement risk, not only to marine megafauna but also to smaller species such as fishes and diving birds, would increase significantly with the size and surface area of the net. This scenario would also be detrimental to the mooring itself, and further investigation is needed to quantify the likelihood of such an event occurring in areas where ORE devices are likely to be deployed.

The method presented here focuses on three different risk parameters. Other risk parameters could have been added to this study. For example, the volume and mass of the floating device may be considered because it can be of similar size and weight to marine megafauna. In addition to the physical properties of the mooring, it is equally important to consider the biological characteristics and behaviours of different species of marine megafauna to assess which species present a higher risk of entanglement. This work has been performed as part of a wider study in parallel with the moorings assessment [31].

Due to the large degree of uncertainty because of the limited experience with the operation of ORE moorings, the rarity of entanglement events and the fact that they are not always detected, these results need to be updated if entanglement is actually observed. From an engineering point of view, this means that mooring systems need to be able to handle the additional weight and volume of a carcass until entanglement can be efficiently monitored or avoided.

6. Conclusion

A methodology has been presented to estimate the relative entanglement risk of marine megafauna with a given mooring configuration. Six different mooring configurations have been used for this study: catenary with chains only, catenary with chains and nylon ropes, catenary with chains and polyester ropes, taut, catenary with accessory buoy, taut with accessory buoy. The parameters which have been used to estimate entanglement risk are tension characteristics, swept volume ratio and mooring line curvature. Taut mooring systems represent the lowest relative risk of entanglement.

The methodology presented in this paper can be used by ORE device developers at the early stage of the mooring design if it is integrated in EIA reporting process. It can also be used for analysis with other mooring configurations, or for power cables or array configurations. There are still uncertainties about the relative importance of the risk parameters, and as projects are deployed and empirical evidence is collected, this uncertainty can be refined.

7. Acknowledgments

The authors gratefully acknowledge the support of Scottish National Heritage, who funded this study.

8. References

- [1] D. Ingram, G.H. Smith, C. Bittencourt-Ferreira, H. Smith (Eds.), *Protocols for the Equitable Assessment of Marine Energy Converters*, University of Edinburgh, School of Engineering Publishers, Edinburgh, 2011.
- [2] S. Benjamins, W. Ledwell, J. Huntington, A.R. Davidson, Assessing changes in numbers and distribution of large whale entanglements in Newfoundland and Labrador, Canada. *Marine Mammal Science*. 28 (2012) 579-601.
- [3] D. Pemberton, N. Brothers, G. Copson, Predators on marine fish farms in Tasmania. *Papers and Proceedings of the Royal Society of Tasmania*. 125 (1991) 33-35.
- [4] B.D. Lloyd, Potential effects of mussel farming on New Zealand's marine mammals and seabirds: a discussion paper. Department of Conservation, Wellington, NZ, 2003.
- [5] A.J. Read, P. Drinker, S. Northridge, Bycatch of marine mammals in U.S. and global fisheries, *Conservation Biology*, 20 (2006) 163-169.
- [6] T.I. Walker, Can shark resources be harvested sustainably? A question revisited with a review of shark fisheries, *Marine and Freshwater Research*, 49 (1998) 553-572.
- [7] A. Cosandey-Godin, A. Morgan, Fisheries bycatch of sharks: Options for mitigation, *Ocean Sciences series*, 2011.
- [8] A. Copping, G. Cada, J. Roberts, M. Bevelhimer, Accelerating Ocean Energy to the Marketplace –Environmental Research at the U.S. Department of Energy National Laboratories, in: *Proc of the 3rd International Conference and exhibition on Ocean Energy (ICOE)*, 2010.
- [9] R.E. Harris, L. Johanning, J. Wolfram, Mooring systems for wave energy converters: A review of design issues and choices, in: *Proc of the 3rd International Conference on Marine Renewable Energy (MAREC)*, 2004.
- [10] D.T. Brown, S. Mavrakos, Comparative study on mooring line dynamic loading, *Marine Structures*. 12 (1999) 131-151.
- [11] J. Cruz, *Ocean Wave Energy Current Status and Future Perspectives*, Springer-Verlag, Berlin, 2008.
- [12] Orcina, Dynamic analysis and control of offshore marine systems using OrcaFlex, presentation to the SUPERGEN 7th Doctoral Training Programme Workshop 'Control of Wave and Tidal Energy Converters', Lancaster University, 2010.
- [13] L. Johanning, G.H. Smith, Station keeping study for WEC devices including compliant chain, compliant hybrid and taut arrangement, in: *Proc. of the 27th International Conference on Offshore Mechanics and Arctic Engineering (OMAE)*, 2008.
- [14] J. Fitzgerald, L. Bergdahl, Considering Mooring Cables for Offshore Wave Energy Converters, in: *Proc of the 7th European Wave and Tidal Energy Conference (EWTEC)*, 2007.
- [15] M. Masciola, A. Robertson, J. Jonkman, F. Driscoll, Investigation of a FAST-OrcaFlex Coupling Module for Integrating Turbine and Mooring Dynamics of Offshore Floating Wind Turbines, in: *Proc of the International Conference on Offshore Wind Energy and Ocean Energy (ICOWEOE)*, 2011.
- [16] Orcina, OrcaFlex manual, version 9.7b, 2014.
- [17] J. C.C. van Nieuwkoop, H.C.M. Smith, G. H. Smith, L. Johanning, Wave resource assessment along the Cornish coast (UK) from a 23-year hindcast dataset validated against buoy measurements, *Renewable Energy*, 58 (2013), 1–14.
- [18] B. Cahill, Characteristics of the wave energy resource at the Atlantic marine energy test site, PhD Thesis, University College Cork, 2013.
- [19] Pelamis, Development history. Last accessed: 23/05/2014. [Online]. Available: <http://www.pelamiswave.com/development-history>

- [20] A. Babarit, J. Hals, M.J. Muliawan, A. Kurniawan, T. Moan, J. Krokstad, Numerical benchmarking study of a selection of wave energy converters, *Renewable Energy*, 41 (2012), 44–63.
- [21] J. Lavelle J. P. Kofoed, Power Production Analysis of the OE Buoy WEC for the CORES Project, The CORES EU Project, DCE Technical Report, No. 119, 2011.
- [22] J. Sjolte, I. K. Bjerke, G.Tjensvoll, M. Molinas, Summary of Performance After One Year of Operation with the Lifesaver Wave Energy Converter System, in: Proc of the 10th [European Wave and Tidal Energy Conference](#) (EWTEC), 2013.
- [23] Carnegie, CETO Commercial Scale Unit Overview. Last accessed: 23/05/2014. [Online]. Available: <http://www.carnegiwave.com/index.php?url=/ceto/ceto-overview>,
- [24] Ocean Power Technologies, OPT MARK 3PowerBuoy, Utility Power from Ocean Waves, Last accessed: 23/05/2014. [Online]. Available: http://www.oceanpowertechnologies.com/PDF/OPT_Mark%203_Feb2014.pdf
- [25] EMEC, Wello Oy, Last accessed: 23/05/2014. [Online]. Available: <http://www.emec.org.uk/about-us/wave-clients/wello-oy/>
- [26] Statoil, Hywind, Crossing energy frontiers, Last accessed: 23/05/2014. [Online]. Available: <http://www.statoil.com/en/TechnologyInnovation/NewEnergy/RenewablePowerProduction/Offshore/Hywind/Downloads/Hywind%20postcard.pdf>
- [27] Principle, Windfloat, Last accessed: 23/05/2014. [Online]. Available: <http://www.principlepowerinc.com/products/windfloat.html>
- [28] EMEC, Bluewater Energy Services, Last accessed: 23/05/2014. [Online]. Available: <http://www.emec.org.uk/about-us/our-tidal-clients/bluewater-energy-services/>
- [29] M. A. Stefanovich, J. Fernández Chozas, Toward Best Practices for Public Acceptability in Wave Energy: Issues Developers Need to Address, in: Proc of the 3rd International Conference and exhibition on Ocean Energy (ICOE), 2010.
- [30] EMEC, Environmental Impact Assessment (EIA); Guidance for developers at the European Marine Energy Centre, 2008.
- [31] S. Benjamins, V. Harnois, H.C.M. Smith, L. Johanning, L. Greenhill, C.Carter, B. Wilson, Understanding the potential for marine megafauna entanglement risk from renewable marine energy developments, Scottish Natural Heritage Commissioned Report, In press.